

Figure S1 | Transcriptomic analysis of cells sorted by cell size

Related to Figures 1D-F.

(A-E) Cells in S/G2/M were sorted into four different bins based on the intensity of a total protein dye that we used as a proxy for cell size. See STAR Methods for further details.

(A) Protein dye intensity (normalized to the mean) measured during sorting (blue) and re-measured for cells from each bin after the sort (yellow). The re-analysis (yellow) confirms high sort fidelity.

(B) The amount of mRNA (mean \pm SEM) per cell for each bin, determined by the number of reads relative to those from a fixed number of *S. pombe* spike-in cells added to the sample. Total protein amount is well correlated with total cellular mRNA amount.

(C-E) Cell volume of cells after sorting, measured by Coulter counter. Total protein amount is correlated with cell volume.

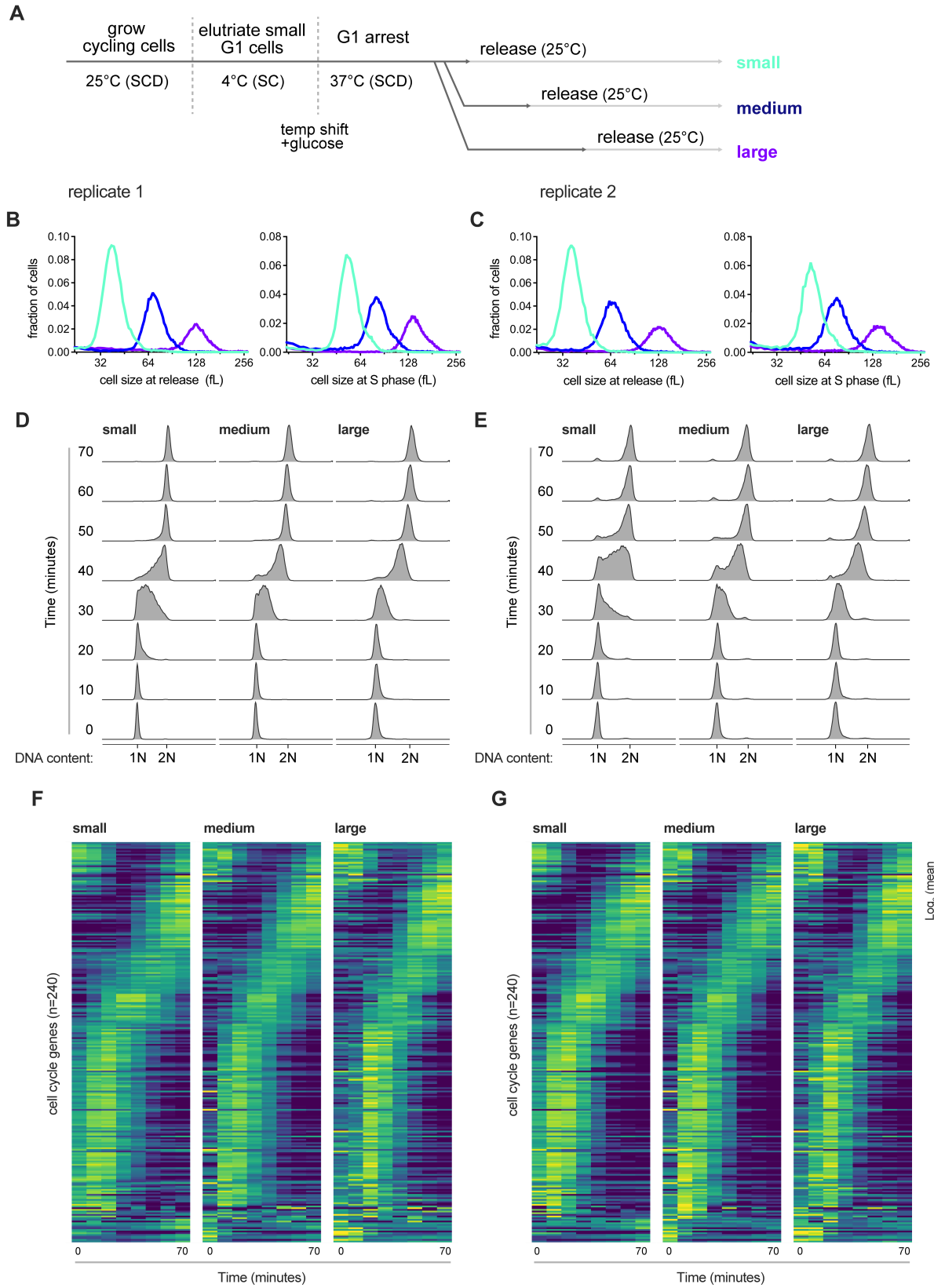


Figure S2 | Transcriptomic analysis of different sized cells synchronously progressing through the cell cycle

Related to Figure 2.

(A) Schematic of experimental design. G1 cells harboring a temperature sensitive Cdk1 allele (*cdc28-13*) were recovered by centrifugal elutriation. Cells were then shifted to the restrictive temperature (37°C) to arrest them in G1. After increasing amounts of time during the arrest, cells reached small, medium or large cell sizes. The culture was then shifted to the permissive temperature (25 °C) to allow cell cycle entry. Samples for RNA-seq were then collected every ten minutes between G1 and cell mitosis. See STAR Methods for further details.

(B&C) Cell size distributions, measured by Coulter counter, for small, medium, and large cells when they are released from the G1 arrest (left panel) or at mid S-phase (the 40-minute time point, right panel) for two biological replicates.

(D&E) DNA content analysis of small, medium, and large cells synchronously progressing through the cell cycle for two biological replicates.

Data in Figures S2B&D are also presented in Figure 2A&B (Shown here for comparison with S2C&E).

(F&G) Heatmap showing the log₂ mean normalized TPM of all high confidence cell cycle regulated genes (de Lichtenberg et al., 2005; Spellman et al., 1998). Yellow corresponds to increase and blue to decrease. Each row corresponds to a single gene. Each column represents a single time point (0-70 minutes). Each heatmap represents a single time-course for the cells of the indicated size.

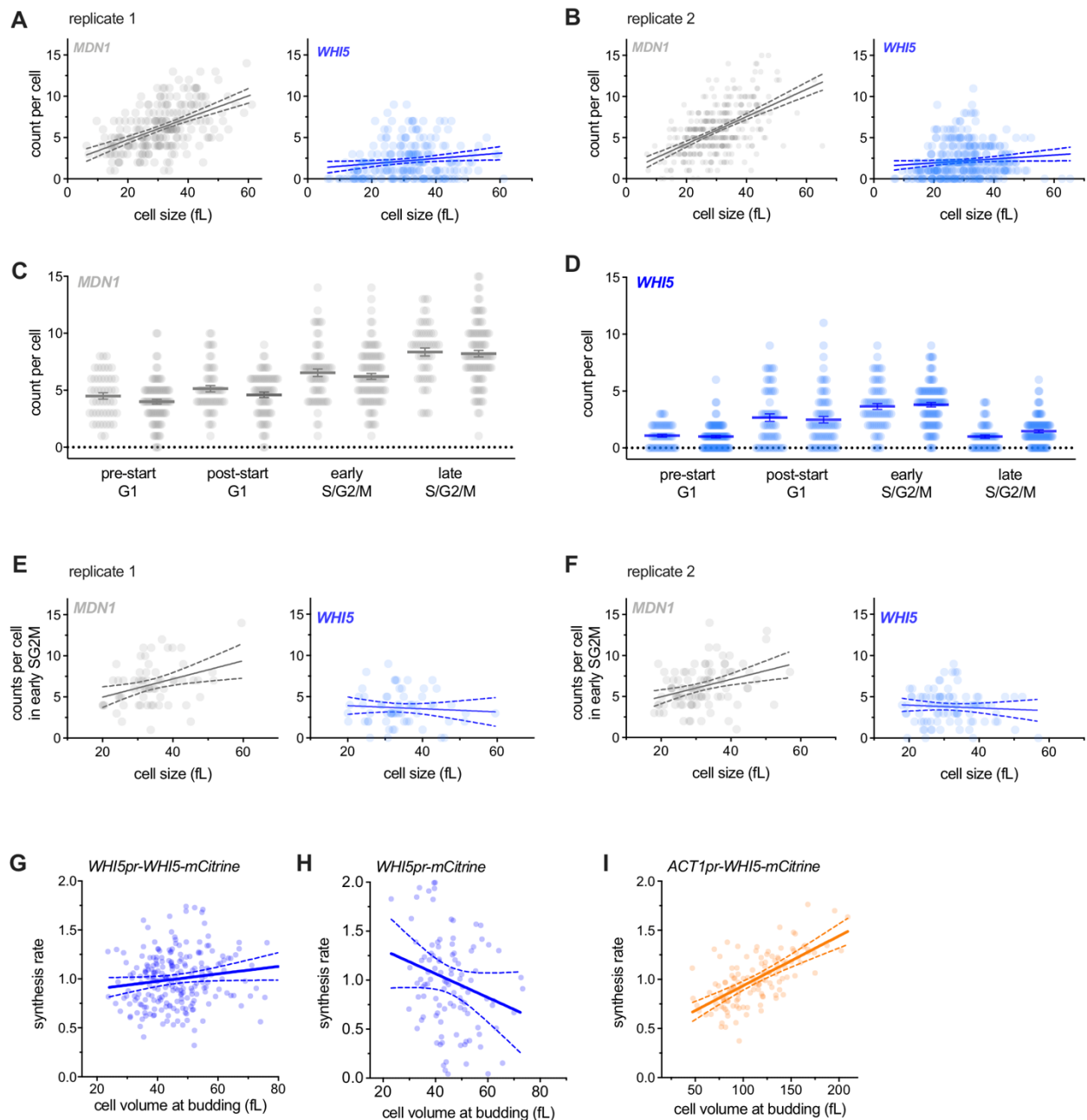


Figure S3 | Single-cell analysis of *WHI5* mRNA expression

Related to Figures 1G-I & 2E-H.

(A&B) mRNA counts per cell, measured by single molecule FISH, for *MDN1* or *WHI5* as a function of cell size in two independent biological replicates. All cells of any cell cycle stage are included. Linear regression (solid line) and 95% confidence interval (dashed lines) are shown. The same data are re-plotted in Fig. 1 H&I with replicates pooled.

(C&D) mRNA counts per cell, measured by single molecule FISH, for *MDN1* or *WHI5* at different cell cycle stages in two independent biological replicates. Mean (solid line) \pm SEM (error bars) are shown. See STAR Methods for details of cell cycle stage classification.

(E&F) mRNA counts per cell, measured by single molecule FISH, for *MDN1* and *WHI5* as a function of cell size during early S/G2/M in two independent biological replicates. Early S/G2/M cells were defined as budded cells with a small (≤ 0.2) bud-to-mother volume ratio. Linear regression (solid line) and 95% confidence interval (dashed lines) are shown. The same data are re-plotted in Fig. 2E with replicates pooled.

(G-I) Protein synthesis rates (normalized to the mean) as a function of cell volume at budding, measured by time-lapse microscopy for Whi5-mCitrine fusion proteins expressed from (G) the endogenous *WHI5* promoter or (I) the *ACT1* promoter and (H) mCitrine expressed alone from the *WHI5* promoter. Synthesis rates were determined for single cells for the period between bud emergence and cytokinesis using a linear fit as in (Schmoller et al., 2015). Linear regression (solid line) and 95% confidence interval (dashed lines) are shown. (G) $n=229$, 2 data points outside the axis limits. (I) $n=113$, 4 data points outside the axis limits. (H) $n=132$. The same data, binned by cell volume at budding, are shown in Fig. 2F-H.

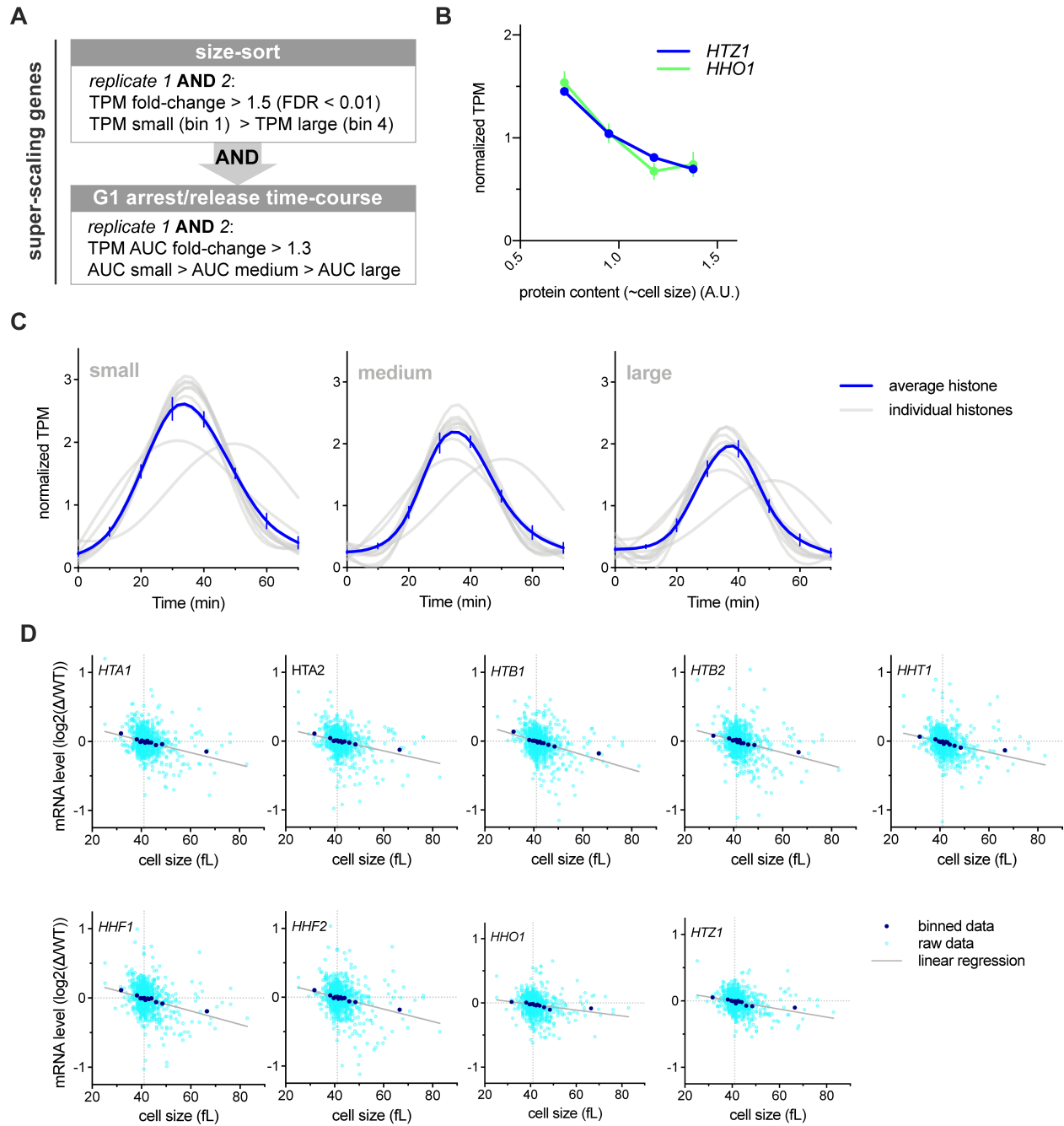


Figure S4 | Histone gene expression sub-scales with cell size

Related to Figure 3.

(A) Criteria used to classify sub-scaling transcripts. Genes whose expression changed in a manner similar to *WHI5* in both replicates of the size-sort (see Fig. 1D-F) and in the G1 arrest/release time course (see Fig. 2A-D) were classified as sub-scaling genes. See STAR Methods for further details.

(B) Normalized TPM (TPM / mean TPM) for *HTZ1* and *HHO1* mRNA in cells of different sizes (total protein content). Mean (\pm range) of two biological replicates is plotted. Changes in TPM are proportional to changes in mRNA concentration. See Figure S1 and STAR Methods for further details.

(C) Normalized histone mRNA TPM (TPM / mean TPM) of small, medium or large cells at 10-minute time intervals synchronously progressing through the cell cycle. A smoothing spline fitted to the mean normalized TPM from two biological replicates for each histone is plotted in grey. A Spline fitted to mean (\pm SEM) of all histones is shown in blue.

(D) Comparison of histone mRNA levels in 1,484 gene deletions, relative to wild-type (Kemmeren et al., 2014; O'Duibhir et al., 2014) with cell size of the respective gene deletions (Jorgensen et al., 2002). Each graph plots a single transcript and each point represents a single gene deletion. See STAR Methods for details. Distribution of Pearson R correlation coefficients for all genes in is show in Fig. 3E.

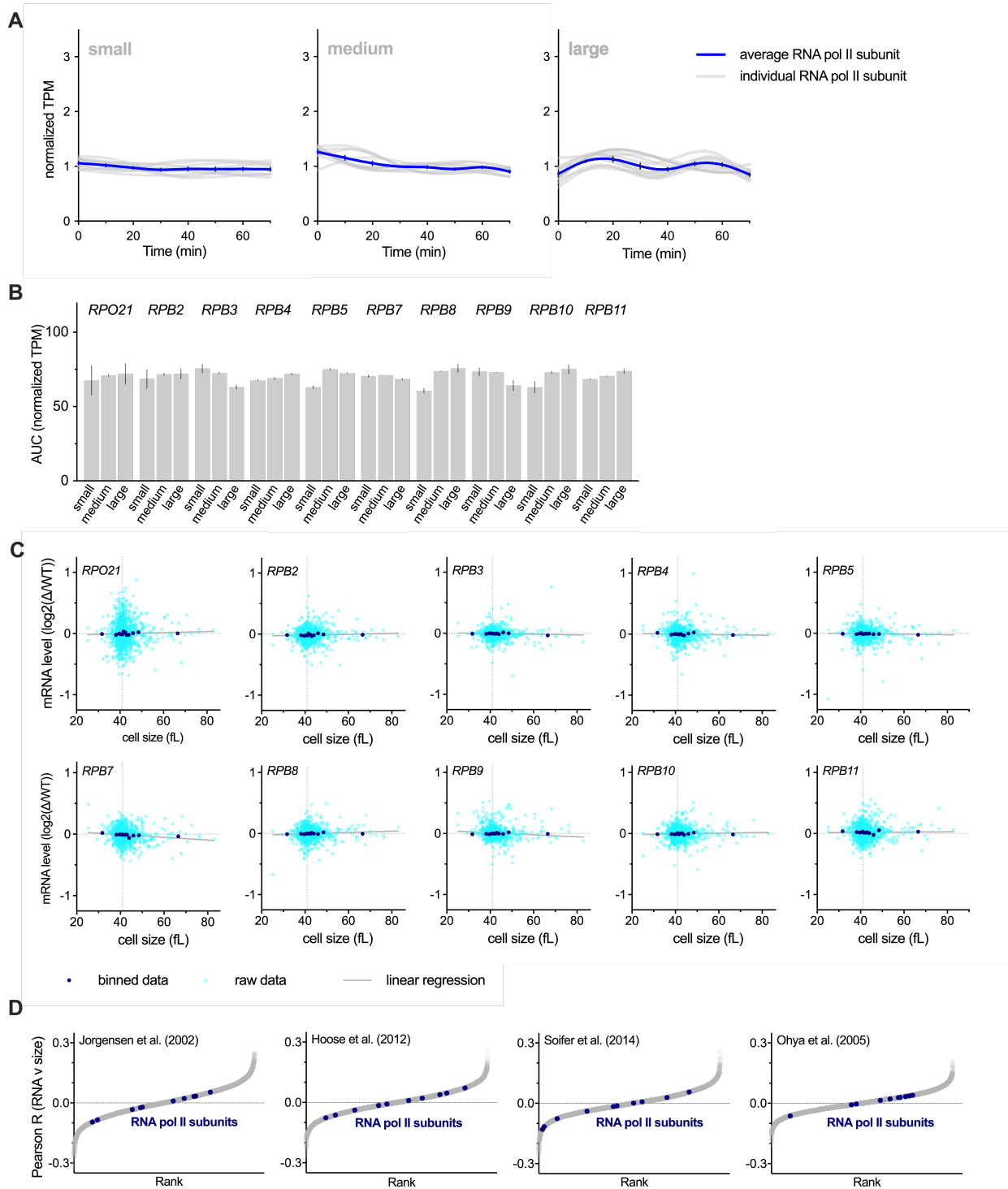


Figure S5 | RNA polymerase II subunit gene expression scales and is proportional to cell size

Related to Figure 3

(A) Normalized RNA polymerase II subunit mRNA TPM (TPM / mean TPM) for small, medium, and large cells at 10-minute time intervals synchronously progressing through the cell cycle. A smoothing-spline fitted

to the average normalized TPM from two biological replicates for each subunit is plotted in grey. A Spline fitted to the mean (\pm SEM) of all subunits is shown in blue.

(B) The Area Under the Curve (AUC) of mean normalized RNA polymerase II subunit mRNA TPM of small, medium, and large cells synchronously progressing through the cell cycle. The AUC mean (\pm range) of two biological replicates is plotted.

(C) Comparison of RNA polymerase II subunit mRNA levels in 1,484 gene deletions (Kemmeren et al., 2014; O'Duibhir et al., 2014) with cell size of the respective gene deletions (Jorgensen et al., 2002). Each graph plots a single transcript and each point represents a single gene deletion. See STAR Methods for details.

(D) Pearson correlation coefficient, R , for the correlation between mRNA levels in 1,484 gene deletion strains (Kemmeren et al., 2014; O'Duibhir et al., 2014) and the cell size of the respective gene deletions for four different data sets of size measurements (Hoose et al., 2012; Jorgensen et al., 2002; Ohya et al., 2005; Soifer and Barkai, 2014). Each point represents an individual gene. RNA polymerase II subunit mRNAs are shown in blue. See STAR Methods for details.

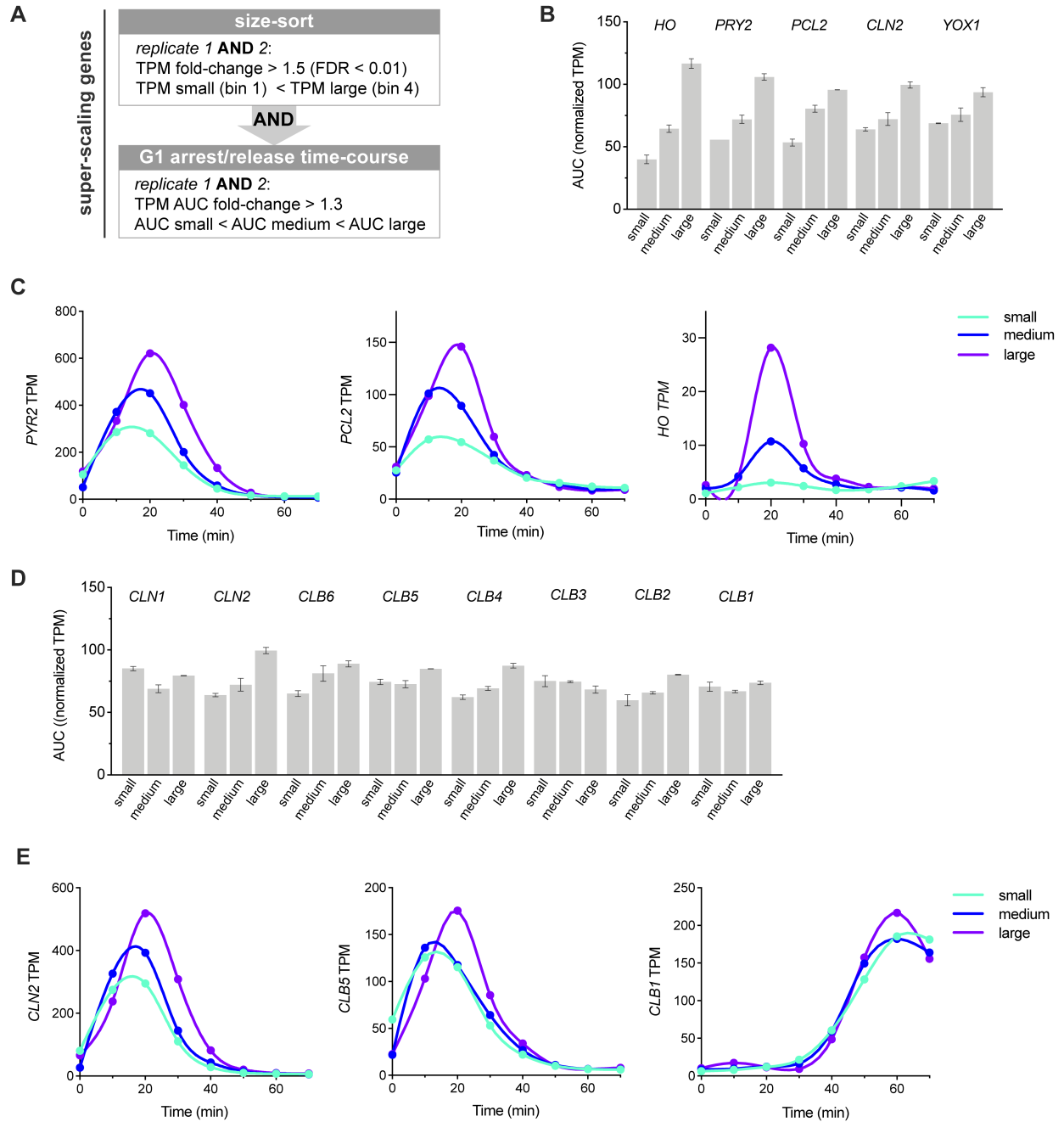


Figure S6 | SBF regulated super-scaling genes and cyclin expression during the cell cycle in cells of different sizes

Related to Figure 3.

(A) Criteria used to classify genes with super-scaling transcript amounts. Genes whose expression increased in both replicates of the size-sort and in the G1 arrest/release time course were classified as super-scaling genes. See STAR Methods for further details.

(B) The Area Under the Curve (AUC) of mean normalized TPM of small, medium, and large cells synchronously progressing through the cell cycle for SBF-regulated super-scaling transcripts. See Fig. S2 for experimental details. The AUC mean (\pm range) of two biological replicates is plotted.

(C) SBF-regulated super-scaling genes TPM for small, medium, and large cells synchronously progressing through the cell cycle. Data for one representative replicate is plotted.

(D) The Area Under the Curve (AUC) of mean normalized TPM of small, medium, and large cells synchronously progressing through the cell cycle for cyclin transcripts. The AUC mean (\pm range) of two biological replicates is plotted.

(E) Cyclin transcript TPM for small, medium, and large cells synchronously progressing through the cell cycle. See Fig. S2 for experimental details. Data for one representative replicate is plotted.

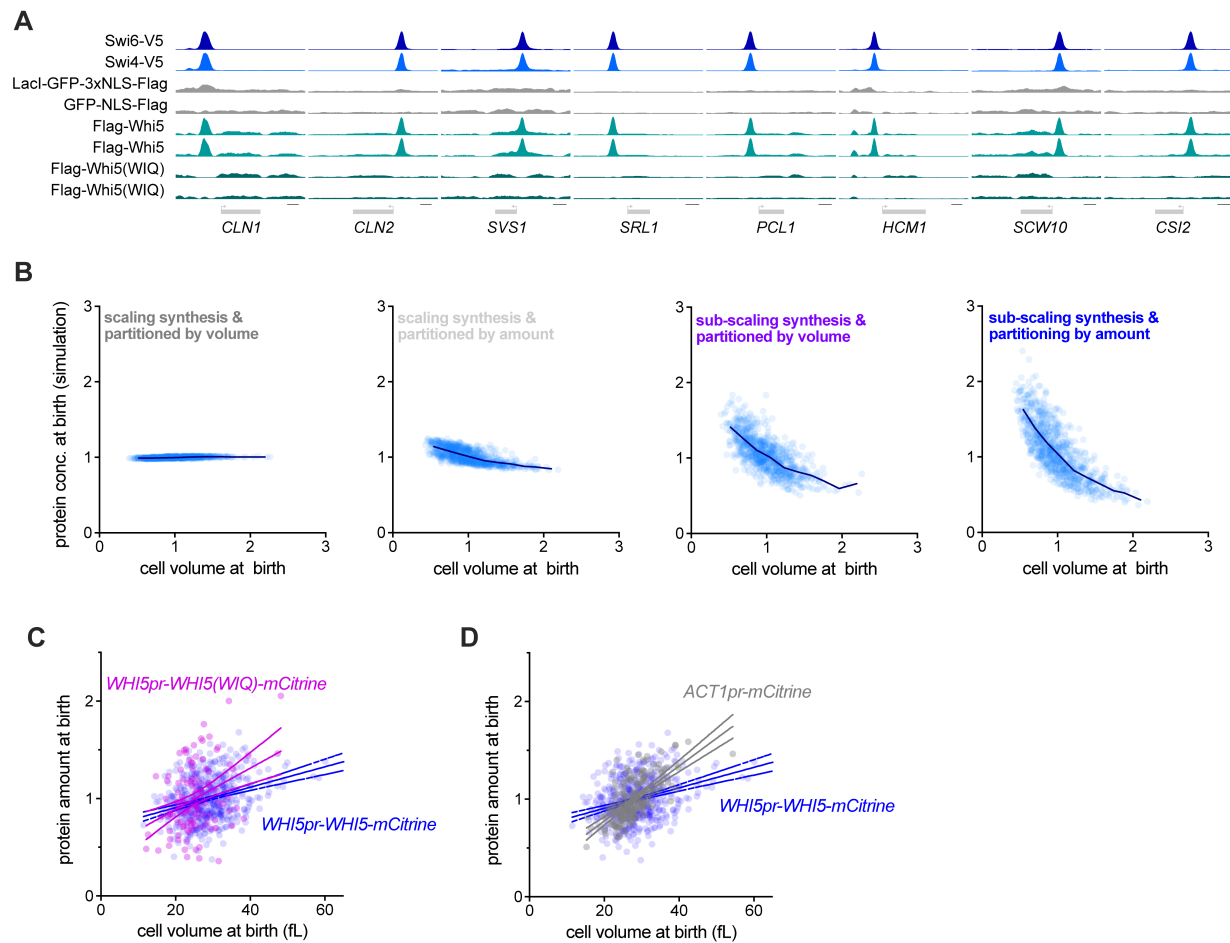


Figure S7 | Sub-scaling expression is inherited through asymmetric division due to DNA-mediated partitioning

Related to Figure 5.

(A) anti-V5 or anti-Flag ChIP-seq experiments were performed using cells expressing the indicated fusion proteins (left hand side). Data are shown for 8 example SBF binding sites near the denoted genes. Cells expressing Lacl-GFP-3xNLS-FLAG or GFP-NLS-FLAG were included as controls for non-specific ChIP signal. Whi5 recruitment to DNA overlaps with SBF (Swi4 and Swi6) binding sites but is lost in the Whi5(WIQ) variant (Travesa et al., 2013). Summary metagene plots for a subset of these data are also shown in Fig. 5C.

(B) Simulated protein concentration at birth as a function of daughter volume at birth. Four different conditions were simulated where protein expression was either in proportion to cell size (scaling) or independent of cell size (sub-scaling), and protein partitioning is either by amount or in proportion to cell volume. Individual simulated cells (light blue) as well as bin means (dark blue) are plotted. Protein amounts from the same simulation are shown in Fig. 5D.

(C&D) Protein amount in daughter cells at birth for the following genotypes: *WHI5pr-WHI5-mCitrine* and (C) *WHI5pr-WHI5(WIQ)-mCitrine* or (D) *ACT1pr-mCitrine*. Linear regression (solid line) and 95% confidence interval (dashed lines) are shown.

Note, Fig. 5E shows bin means of the same data as (C) binned by cell volume at birth.

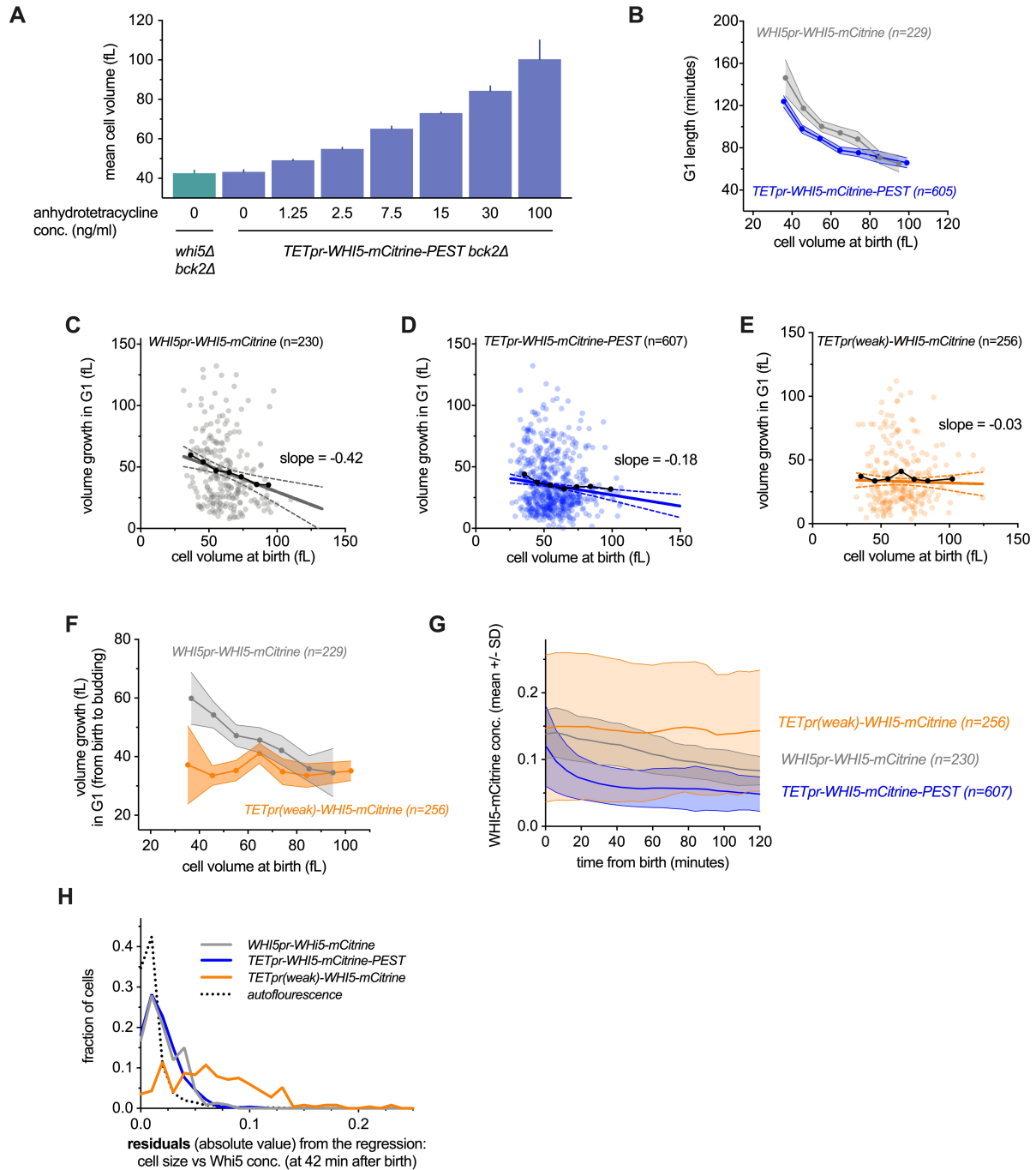


Figure S8 | Disruption of Whi5 sub-scaling expression

Related to Figure 6.

(A) Cell size, determined by coulter counter, of the indicated genotype at different anhydrotetracycline concentrations. Mean (\pm SEM) of three independent biological replicates is shown.

(B) Time in G1 as a function of cell size at birth for daughter cells with a completed G1. Data are binned according to cell size at birth for cells with a completed G1 and the bin means (\pm SEM) are plotted.

(C-E) Cell volume growth in G1 (birth to budding) plotted against cell volume at birth for the following genotypes: (C) *WHI5pr-WHI5-mCitrine bck2Δ*, (D) *TETpr-WHI5-mCitrine-PEST bck2Δ*, and (E) *TETpr(weak)-WHI5-mCitrine bck2Δ*. Linear regression (solid line) and 95% confidence interval (dashed lines) are shown. Bin means (black dots) are also shown. Linear regressions are calculated after outlier removal (Q=1%), which resulted in 2 (C), 7 (D) and 2 (E) cells being excluded respectively. Note, Fig. 6D and Fig. S8F shows bin means of the same data binned by cell volume at birth.

(F) Cell growth in G1 as a function of cell volume at birth for daughter cells that completed G1. Data are binned according to cell volume at birth and the bin means (\pm SEM) are plotted. Un-binned single-cell values of the same data are plotted in Fig. S8C&E.

(G) Mean Whi5 concentration (\pm standard deviation) as a function of time from birth in all daughter cells that completed G1. *WHI5pr-WHI5-mCitrine bck2Δ* (grey) and *TETpr-WHI5-mCitrine-PEST bck2Δ* (blue) have similar standard deviations around the mean indicating they have similar amounts of gene expression noise. In contrast *TETpr(weak)-WHI5-mCitrine bck2Δ* (orange) has a larger standard deviation and increased gene expression noise.

(H) Histogram of the absolute values of residuals ($\sqrt{r^2}$) from the linear regression between Whi5 concentration and cell volume at a fixed timepoint in early G1 (42 minutes after birth) for all daughter cells that completed G1 of the indicated genotypes. Larger residuals correspond to larger gene expression noise. *WHI5pr-WHI5-mCitrine bck2Δ* (grey; median = 0.017) and *TETpr-WHI5-mCitrine-PEST bck2Δ* (blue; median = 0.016) are less noisy than *TETpr(weak)-WHI5-mCitrine bck2Δ* (orange; median = 0.064). Linear regression to cell volume was used to ensure that the size-dependent variation in Whi5 concentration does not confound our estimate of gene expression noise. The residuals for the same regression for an untagged background control strains (dashed line; median = 0.007) was calculated for all cells and corresponds to noise due to auto-fluorescence.

Table S1 – List of *S. cerevisiae* strains used in this study and full genotypes

Related to STAR Methods

A17896	Amon lab	<i>W303; MATa, ADE2, cdc28-13</i>
DCB99	This study	<i>W303; MATa, ADE2, WHI5-mCitrine::URA3</i>
MK551-1	This study	<i>W303; MATa, bar1Δ::HisG, whi5Δ::LEU2, cln3Δ::hphMX6</i>
MS118	This study	<i>W303; MATalpha, ADE2, HTB2-sfGFP::HisMX6, myo1-3xmKate2::kanMX6</i>
MS120	This study	<i>W303; MATalpha, ADE2, HTA2-sfGFP::HisMX6, myo1-3xmKate2::kanMX6</i>
HTB2-GFP	GFP collection (Huh et al., 2003)	<i>BY4741; HTB2-GFP</i>
DCB72	This study	<i>W303; MATa, ADE2, ura3:: WHI5pr(1kb)-mCitrine-CYC1term</i>
KSY108-1	Lab collection	<i>W303; ADE2, WHI5-mCitrine-HIS3</i>
KSY190-2	This study	<i>W303; ADE2, whi5Δ::KanMX6 URA3::WHI5pr(1kb)-WHI5-WIQ-mCitrine-ADH1term</i>
KSY160-2	This study	<i>W303; ADE, URA3::ACT1pr(1kb) -Whi5-mCitrine-CYC1term</i>
KSY158-1	Lab collection	<i>W303; ADE2, URA3:: ACT1pr(1kb)-mCitrine-CYC1term</i>
MS534	This study	<i>W303; bar1Δ::HisG, URA3::GFP-3xNLS-FLAG</i>
MS535	This study	<i>W303; bar1Δ::HisG, URA3::LacI-GFP-3xNLS-FLAG</i>
MS536	This study	<i>W303; bar1Δ::HisG, whi5Δ::LEU2, URA3::WHI5pr(1kb)-3xFLAG-WHI5-CYC1term</i>
MS537	This study	<i>W303; bar1Δ::HisG, URA3::WHI5pr(1kb)-3xFLAG-WHI5(WIQ)-CYC1term</i>
MK653-1	This study	<i>W303; bar1Δ::HisG, SWI4-V5::hphMX6</i>
MK645-1	This study	<i>W303; bar1Δ::HisG, SWI6-V5::hphMX6</i>
MS364	This study	<i>W303; MATalpha, ADE whi5Δ::cgTRP; bck2Δ::hphNT1, myo1-3xmKate2::kanMX6, leu1::PtetO7.1-WHI5-mCitrine-PEST::LEU1, WTC846(PrtetO-7.1-TetR, PrRNR2-TetR-TUP1)::HIS3</i>
MS367	This study	<i>W303; MATalpha, ADE, whi5Δ::cgTRP; bck2Δ::hphNT1, myo1-3xmKate2::kanMX6, WHI5pr[1kb]-WHI5-mCitrine::URA3, WTC846(PrtetO-7.1-TetR_PrRNR2-TetR-TUP1)::HIS3</i>
MS391	This study	<i>W303; MATalpha, ADE, whi5Δ::cgTRP; bck2Δ::hphNT1, myo1-3xmKate2::kanMX6, leu1::PtetO7.1(weak)-WHI5-mCitrine::LEU1, WTC846(PrtetO-7.1-TetR, PrRNR2-TetR-TUP1)::HIS3</i>